

# EXPERIMENTAL STUDY OF A VARIABLE BUOYANCY SYSTEM FOR LOW DEPTH OPERATION

Reference NO. IJME 1203, DOI: 10.5750/ijme.v165iA1.1203

**B K Tiwari<sup>1,\*</sup>, R Sharma<sup>2</sup> and Tae-wan Kim<sup>3</sup>**

<sup>1,3</sup>Department of Naval Architecture and Ocean Engineering, Research Institute of Marine Systems Engineering, Seoul National University, Seoul, Republic of Korea.

<sup>2</sup>Design and Simulation Laboratory, Department of Ocean Engineering, Indian Institute of Technology Madras, Chennai (TN) - 600 036, India  
E-mails: \*bktiwari@snu.ac.kr; rajivatri@iitm.ac.in, taewan@snu.ac.kr

KEY DATES: Submission date: 16.07.22 / Final acceptance date: 12.05.23

## SUMMARY

Autonomous Underwater Vehicles (AUVs) are used for underwater surveying both in coastal areas and deep sea without human intervention during their operations. AUV's performance, including range and endurance, is adversely affected by their high energy consumption by their thrusters. Herein, we have presented a novel design and development of a standalone variable buoyancy system for an autonomous underwater vehicle. We have studied the numerical and experimental analysis of Variable Buoyancy System (VBS) in standalone mode. Design idea is based upon the 'Pump Driven Variable Buoyancy System (PDVBS)' using 'Water Hydraulic Variable Buoyancy System (WHVBS)' method to control buoyancy using a diaphragm type positive displacement pump (PDP) with maximum buoyancy change capacity at a rate of 4.5 kg/min. An in-depth investigation of the performance of the developed VBS has been conducted both experimentally and in simulation. Linear regression analysis has been investigated and the performance of the Linear Regression Model (LRM) is evaluated based on the computation of the Root Mean Square Error (RMSE) of the LRM. The developed VBS is tested at maximum depth of 5 m and compared to experimental and simulation results. Presented results demonstrate that the designed VBS is effective at changing buoyancy and controlling heave velocities. This will result in achieving higher range and endurance and better performance in rescue/attack operations.

## NOMENCLATURE

$\alpha$	Learning rate
$\theta_0, \theta_1$	Training parameter
$\rho$	Fluid density (kg-m <sup>-3</sup> )
$A_p$	Projected area (m <sup>2</sup> )
$a$	Acceleration of the system (m-s <sup>-2</sup> )
$\Delta B$	Change in buoyancy (N)
$C_D$	Drag coefficient
$F_G$	Gravitational force (N)
$F_B$	Buoyancy force (N)
$g$	Gravitational acceleration (m-s <sup>-2</sup> )
$m$	Mass of developed buoyancy system (kg)
$m_a$	Added mass (kg)
$n_t$	Total number of training data
$V_d$	Displaced volume (m)
$w$	Heave velocity (m-s <sup>-1</sup> )

AUV	Autonomous Underwater Vehicles
DSV	Deep Submergible Vehicles
DWF	Deep Water Flume
HOV	Human Occupied Vessels
LR	Learning Rate
LRM	Linear Regression Model
ML	Machine Learning
PDDP	Positive Displacement Diaphragm Pump
PoC	Proof of Concept
RMSE	Root Mean Square Error
ROV	Remotely Operated Vehicles

URV	Underwater Robotic Vehicle
VBS	Variable Buoyancy System
WHVBS	Water Hydraulic Variable Buoyancy System

## 1. INTRODUCTION

The exploration of the ocean remains a challenging area for various applications, such as oil and gas exploration, underwater surveying, shipping, and deep-sea mining. Table 1 shows the classification of various underwater vehicles. From the existing literature it can be observed that the high energy consumption by underwater vehicles will reduce the operational range and endurance of the vehicle. If energy storage capacity is increased, it will adversely affect vehicle payload capacity. So, to overcome these challenges, an alternative method i.e. to control the net buoyant force acting on the vehicle was conceived by researchers at different organizations. A vehicle's buoyancy can be controlled through two methods: 1) active buoyancy control, which is achieved either by changing its mass in every cycle, or 2) passive buoyancy control, in which dead weight is used to control buoyancy.

Kojima et al. (1997) has discussed AQUA EXPLORER-2 that uses two dead weights, each of two kg for improving the safety and reliability of the vehicle and Desset et al. (2005) discussed simulation study of ODYSSEY AUV with active thrust controller and 10 kg of drop of dead weight which gives it vertical speed of 3.5 m/s. Although

these passive methods of buoyancy control are applicable for fast release/recovery, safety and reliability of the UVs but they are not applicable only for one-way buoyancy control and not for cyclic buoyancy control. Davis et al. (2002) has discussed the buoyancy of the Spray glider and Sea glider has been controlled by transfer of the hydraulic fluid between internal and external bladder by using the high-pressure reciprocating hydraulic pumps.

Table 1: Classification of various underwater vehicles

Human Occupied Vessels (HOVs)	Defense Vehicle	Submarines - Its buoyancy can be controlled by using the ballast tanks that can be filled with water or air	- Diesel Electric Low operating range and endurance  - Nuclear Powered High operating range and endurance
		Submersibles	NA
	Research Vessels	Deep Submergence Vehicles (DSV)  - Controls the buoyancy by pumping water into /out of its variable ballast tanks or - By releasing the dead weights  Application: Deep ocean research and rescue	- Trieste/bathyscaphe Control the buoyancy by releasing iron shots to control their descent) Allowed free diving, Operating range-10.9 km - Alvin (DSV-2) Tested for max. operating depth 6.5 km - Sea Cliff (DSV-4) up to 6.1 km
Unmanned Vehicles (UVs)	Remotely Operated	Powered by mother-ship connected by tether/cables  Application: Search and Rescue, Inspection in oil and gas industry, marine science	- Micro/Mini ROVs, Installed with the sensors for underwater system detection, small payload < 2 kg  - Light work class, Payload <200 kg - Heavy work class Payload capacity>200 kg
	Autonomous	Powered (AUVs)  Operated by using propeller/thruster or in hybrid mode (VBS + thruster)	Small, Medium and Large size Buoyancy range: large (up to 90 kg) Speed range: 0.25 – 3.0 m/s
		Unpowered or low powered (Glanders)  VBS control the buoyancy by displaced volume or overall mass of the vehicles	Small and medium size vehicles  Buoyancy range: less than 0.5 kg Speed range: 0.2 –1 .5 m/s

Webb et al. (2001) discussed the design and development of the Slocum glider which used a single-stroke pump with a rolling diaphragm seal to control buoyancy by

pumping seawater into or out of the ballast tank. Although, the performance of these buoyancy control systems is excellent for gliders, they can only be utilized for very small buoyancy changes.

Kobayashi et al. (2011) discussed the VBS for deep water operation by using the single-stroke piston by injection/extraction of the hydraulic oil to or from the external bladder and controlling the buoyancy by control in the total displaced volume by the vehicles. Shibuya et al. (2013) discussed the change in the buoyancy by changing the displaced volume of the metal bellows (which is able to withstand high water pressure) using the paraffin wax and changing phase from solid to liquid phases and vice-versa by heating or cooling the paraffin box. Ranganathan et al. (2017) developed the buoyancy control method by controlling the displaced volume of the metal bellows by operating the linear actuator. But all these methods of buoyancy control are applicable only for the small change in the buoyancy capacity.

Sumantr et al. (2008) has discussed the simulation performance of ‘Underwater Robotic Vehicle (URV)’ used to control the buoyancy of the system by movable plate inside the ballast tank. This resulted in the change in vehicle buoyancy by changing the volume of the ballast tank filled with water. This method has the limitation of the high mechanical complexity and no feasibility study and efficiency analysis has been conducted. Thorleifson et al. (1997) discussed a passive buoyancy control system of 95 kg buoyancy capacity for Theseus AUV (used for laying fiber-optic cables in the Arctic sea) and the increase in buoyancy due to cable unspooling can be compensated by filling the seawater surrounding each spool. Tangirala et al. (2007) discussed the buoyancy control system of 90.72 kg buoyancy capacity for the Seahorse AUV. This vehicle can be used for various applications such as environmental monitoring, surveillance, oceanographic survey and seabed mapping. Hyakudome et al. (2002) and Zhao et al (2010) developed the VBS in which buoyancy is controlled by controlling the change in the displaced volume. This system consist oil tank and rubber oil bladder in which oil can be transferred from the tank to bladder and vice-versa to control the buoyancy of the system. Tiwari et al. (2020) presented the detail design and analysis of the VBS development and computer simulation analysis of the AUV in integration with VBS for various designs and scalability analysis. The detailed experimental analysis, however, has not been carried out.

Worall et al. (2007) has developed the VBS for deep operation and is capable of 30 kg of buoyancy change by using an axial piston pump to fill/remove the water to/from the ballast tank. But the experimental performance of their developed VBS has not been reported in standalone mode or in integration with the AUV. Woods et al. (2012) presented a buoyancy system which used both compressed air and the water pump to control the buoyancy; however, in real field

application this is a very complicated mechanism. Huang et al. (2020) discussed the efficient controller for floating ocean seismograph in which variation in buoyancy due to variation in seawater density is addressed and compensated by the control in the displaced volume but in this the detail design of the buoyancy system is not reported.

### 1.1 MOTIVATION AND CONTRIBUTION

From the literature, it appears that there are several systems for buoyancy control, but they either have very large buoyancy capacities that can only be used for large AUV ( $> 8$  m), or have very small buoyancy capacities that can only be used for trimming the vehicles. In addition, the design examples presented by the various researchers to control the buoyancy by controlling the mass change when filling/emptying the ballast tanks are very complex, and best of our knowledge there is no experimental study of the performance of the VBS in the real environment conducted to support their work.

In this paper, we present the detailed experimental study of a unique water hydraulic variable buoyancy system (WHVBS) that can be used for medium size AUVs (i.e., 3 m to 6 m in length). Herein, we investigated the experimental performance of the developed VBS, where we control the net change in buoyancy ( $\Delta B$ ) by filling/discharging water into/from the ballast tank (for more details, see Tiwari et al. (2021)). We compared the experimental results with the simulation results to investigate the feasibility analysis of the developed VBS in standalone mode for proof of concept (PoC).

The remaining part of this paper is organized as follows: Section 2 presents the mechanical components of the developed VBS, Section 3 discusses the mathematical modeling of the VBS in standalone mode, Section 4 presents the experimental results and discussion, and Section 5 presents the conclusions and future work.

## 2. MECHANICAL COMPONENTS OF THE DEVELOPED VBS

In this study, we have developed the complete VBS in standalone mode. The complete design of the VBS is divided into three modular parts. The first part is the lower hemispherical ballast tank, into which water is added or removed from to control buoyancy. The middle part is used to house the pump, solenoid valves, water flow sensors and other electronic accessories, as well as the upper/closed hemispherical parts that form the hydrodynamic shape of the developed VBS to reduce drag. The inner radius of the hemispherical ballast tank is 150 mm, considering the total change in buoyancy capacity  $\pm\Delta B = 5$  kg and 75% of the volumetric efficiency of the ballast tank. The upper closed part of the developed VBS has the same dimensions as the lower hemispherical ballast tank, and the material

selection for the different components is described in our previous work Tiwari et al. (2021).

### 2.1 LEAKAGE TESTING AND INTEGRATION OF THE MODULAR PARTS OF VBS

In this study, to ensure the tightness of the VBS during the integration of the modular parts, we used rubber O-rings placed on both sides of the flange of the hemispherical upper dome and the lower ballast tank. Although the tightness of the system is a challenge for the VBS, as it has to withstand a pressure of 6 bar or more. However, since our test depth is limited to 5.0 m, the seal test at greater depth was not investigated in the current study and may be performed in the near future. However, Table 2 can be used to support the validation and functionality of the pressure and other sensors for the 60 m operating depth. From Table 2, we can see that the specification and operating range of the sensors are from 0.8 MPa to 2.0 MPa (approximately 8 to 20 bar). Thus, if we also consider the lower application range, the performance is better up to a pressure of 6 bar or above. Fig. 1A shows a CAD model of the VBS and Fig. 1B shows the VBS during a test in standalone mode. In Fig. 1A, it can be seen that we used the lower circular rings to compensate for the excess buoyancy caused by the developed VBS in standalone mode, which also serve as stands for the developed VBS.

### 2.2 INTERNAL COMPONENTS AND ELECTRONIC SENSORS

The main internal components of the developed VBS include the pump, flow sensor, unidirectional valves, i.e. solenoid valves, microcontroller and pressure sensor. In this study, we used a diaphragm displacement pump, a 12-V solenoid valve, an Arduino microcontroller, an analog gravity water pressure sensor and a flow sensor.

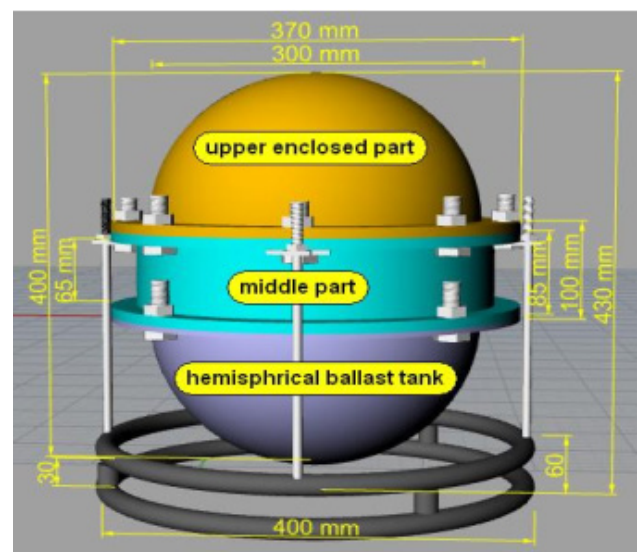


Figure 1: A - CAD model of the VBS.



Figure 1. B- VBS during testing in standalone mode

Table 2 shows the detail specification of the gravity water pressure sensor, solenoid valve, and water flow sensor. Details of the connections of the internal components can be found in our previous publications Tiwari et al. (2021).

Table 2: Specification of the (A) pressure sensor, (B) solenoid valve and (C) flow sensor

(A)	
Type of sensor used	Gravity analog water pressure sensor
Pressure measurement range	0~1.6 MPa
Input voltage	+5 V DC
Output voltage	0.5~4.5 V
Operating temperature	-20~85°C
Normal operating pressure	≤2.0 MPa
Response time	<2.0 ms
(B)	
Operating voltage	12-V DC
Rated current	0.6 Amp
Operating temperature	Maximum 85°C
Normal operating pressure	≤0.8 MPa
Operating mode	Normally closed
(C)	
Model type	YF-S201
Sensor type	Hall effect
Maximum water pressure	2.0 MPa
Working voltage	5 to 18V DC
Working Temperature range	Maximum up to +80°C
Max current draw	15mA
Working flow rate	1 to 30 Liters/Minute
Size	2.5" x 1.4" x 1.4"

### 3. MATHEMATICAL MODELING OF THE DEVELOPED VBS IN STAND-ALONE MODE

From the fundamental of the physics, net change in buoyancy ( $\Delta B$ ) of the submerged vehicles can be defined as following:

$$\Delta B = (W - B)/g = (m - \rho \nabla) \quad (1)$$

where  $W$  is the total weight of vehicle,  $B$  is the buoyancy force of the vehicle,  $\nabla$  is the volume displaced by the vehicle,  $g$  is the gravitational acceleration, and  $\rho$  is the density of fluid. If the net buoyant force  $\Delta B = 0$ , then the vehicle is neutrally buoyant, if  $\Delta B > 0$  then it is positively buoyant and if  $\Delta B < 0$  then the vehicle is negatively buoyant. A mathematical model is developed for the VBS in stand-alone mode to study its performance and the focus is only in one direction, i.e. vertically up/down. Now, the force balance equation can be written as follows:

$$(m + \Delta m)a = F_G - F_B - F_D - F_a, \text{ and} \quad (2)$$

$$(m + \Delta m)a = (m + \Delta m)g - \rho V_d g - \frac{1}{2} C_D \rho A_p |w| w - m_a a \quad (3)$$

where  $m$  is the mass of system,  $\Delta m$  is the change in mass of the system,  $F_G$  is the gravitational force,  $F_B$  is the buoyant force,  $F_D$  is the drag force,  $F_a$  is the force component due to added mass,  $g$  is the gravitational acceleration,  $\rho$  is the fluid density (here we consider fresh water density),  $V_d$  is the displaced volume by the system,  $C_D$  is the drag coefficient,  $A_p$  is the projected area of the VBS,  $w$  is the velocity in vertical plane (i.e. heave velocity),  $m_a$  is the added mass and  $a$  is the acceleration of vehicle is standalone mode. For the neutrally buoyant condition, i.e. when  $\Delta m = 0$  we find  $w = 0$ . So, Equation (3) reduced to the following:

$$(m + \Delta m + m_a)a = \Delta m g - \frac{1}{2} C_D \rho A_p |w| w, \quad (4)$$

$$a = \frac{-0.5 C_D \rho A_p |w| w}{m + \Delta m + m_a} + \frac{\Delta m g}{m + \Delta m + m_a}, \quad (5)$$

$$\dot{w} = \frac{-0.5 C_D \rho A_p |w| w}{m + \Delta m + m_a} + \frac{\Delta m g}{m + \Delta m + m_a}, \quad (6)$$

$$\dot{z} = w \quad (7)$$

Assuming  $\Delta m g = \delta W$  and then the state-space form using the Equation (6) and (7), can be written as the following

$$\begin{bmatrix} \dot{z} \\ \dot{w} \end{bmatrix} = \begin{bmatrix} 0 & 1 \\ 0 & -Z_w \end{bmatrix} \begin{bmatrix} z \\ w \end{bmatrix} + \begin{bmatrix} 0 \\ K_{in} \end{bmatrix} \delta W \quad (8)$$

Where,

$$Z_w = \left( \frac{C_D \rho A_p |w|}{2(m + \Delta m + m_a)} \right) \text{ and } K_{in} = \left( \frac{1}{m + \Delta m + m_a} \right) \quad (9)$$

where  $C_D$  is the drag coefficient,  $\rho$  is the fluid density (here we consider fresh water density),  $A_p$  is projected area of the VBS,  $w$  is the heave velocity in vertical plane,  $m$  is the mass of system,  $\Delta m$  is the change in mass of the system,  $m_a$  is the added mass of the VBS in standalone mode. Simulation parameters of the developed VBS is shown in Table 3. Added mass  $m_a$  is computed based on the assumption made for the designed VBS as prolate ellipsoid shape and can be computed using the following Equation (10), for more details see Fossen T.I. (1994).

$$m_a = Z_w = \left( \frac{-\alpha_0}{2 - \alpha_0} \right) m, \quad (10)$$

where  $\alpha_0 = \frac{2(1 - e^2)}{e^3} \left[ 0.5 \ln \left( \frac{1+e}{1-e} \right) - e \right]$ ,  $e = 1 - \left( \frac{b}{a} \right)^2$  and

$a, b$  are the semi-axes of the prolate ellipsoid shape of the VBS as shown in Fig. 2 and their values are 0.20 m and 0.156 m respectively.

Table 3. Simulation parameters of the VBS in the standalone mode

Parameter	Value	Unit
$m$	26.65	kg
$m_a$	11.2	kg
$A_p$	0.098	m <sup>2</sup>
$C_D$	0.8	-
$g$	9.81	m/s <sup>2</sup>
$\rho$	1000	kg/m <sup>3</sup>
$V_d$	0.026	m <sup>3</sup>

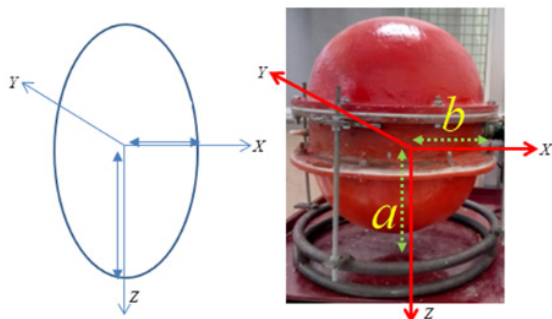


Figure 2. Idealized shape of the designed VBS as a prolate ellipsoid

#### 4. EXPERIMENTAL RESULTS AND DISCUSSION

The performance of the developed VBS in standalone mode was tested in the ‘Deep Water Flume (DWF)’ facility at the Department of Ocean Engineering, Indian Institute of Technology Madras, India. It should be noted that the available water depth in the tank is 5.5 m, so the tests are limited to a maximum depth of 5.0 m to avoid hard landing on the bottom. In addition, it should be noted that all numerical simulations are performed with a fluid assumed to be fresh water, as testing in the sea/ocean/river/lake for standalone mode is difficult and prohibitively expensive due to dependence on a boat/ship and other associated costs. To ensure that the results are verifiable and can be subjected to critical review, the video of the trial can be accessed from VBS Testing (2021). This video has been posted on ‘youtube’ to ensure that the results are available to a wider audience for critical review and evaluation. In this video, it can be clearly seen that the developed VBS starts with a positive buoyancy in the standalone mode and then as the water is filled into the ballast tank, the system acquires a negative buoyancy. In the negative buoyant condition, the mass of the developed VBS in standalone mode is greater than the buoyancy, so the VBS begins to sink. This can be clearly seen on the video. Later, after reaching the desired depth (which is preselected depending on the limitations of the water in the Deep-Water Flume (DWF)), the water is drained from the ballast tank to the external environment. In addition, the mass of water in the ballast tank decreases as the water is released from the ballast tank to the outside, giving the system positive buoyancy and causing the VBS to rise back to the surface. Fig. 3 shows the ascent and descent profiles of the VBS in standalone mode for the buoyancy changes of = 0.2 kg, 0.4 kg, and 0.6 kg, respectively, at 4 m depth. From these results, a depth of 4.0 m is reached in almost 24 s with a buoyancy change of 0.2 kg, and the same depth of 4.0 m is reached in 13 s with the average heave speed of 0.3 m/s and a buoyancy change of 0.6 kg. Similarly, ascending from 4 m depth to the surface, the developed VBS takes the same time to ascend to the surface in standalone mode with the same buoyancy change. Fig. 4 shows the ascent and descent profiles of the VBS for a depth of 5 m with the same amount of buoyancy change as in Fig. 3. From these results, the time required to reach the depth of 5 m with a buoyancy change of 0.2 kg is about 29 s, i.e., with the same average heave speed of about 0.17 m/s, and the same depth of 5 m is reached in 17 s, with an average heave speed of about 0.3 m/s with a buoyancy change of 0.6 kg.

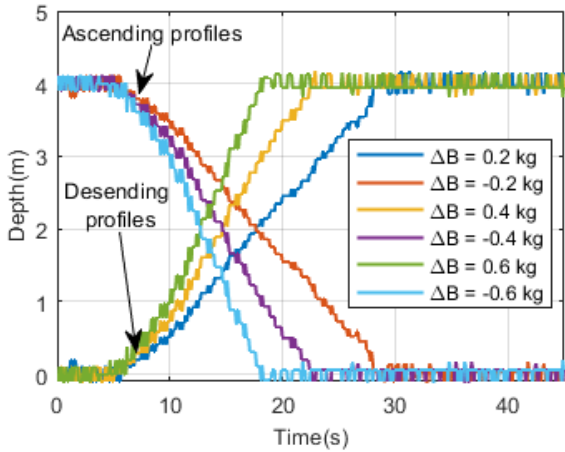
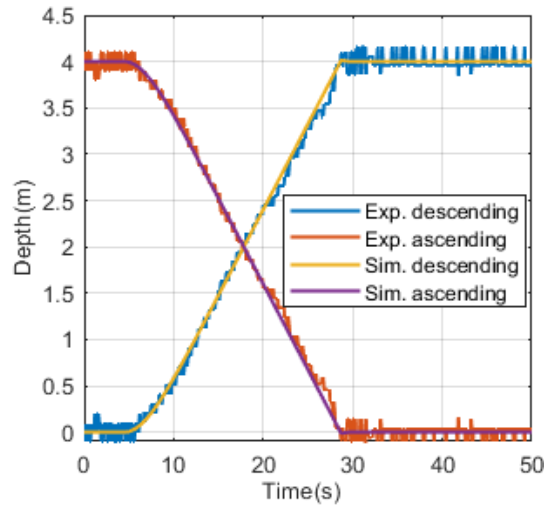


Figure 3. Experimental ascending and descending profile for  $\Delta B = 0.2$  kg, 0.4 kg and 0.6 kg for 4.0 m operating depth of the VBS in standalone mode.



(a)  $\Delta B = 0.2$  kg

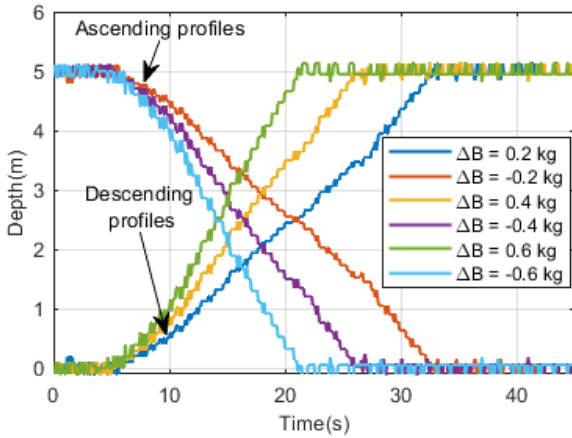
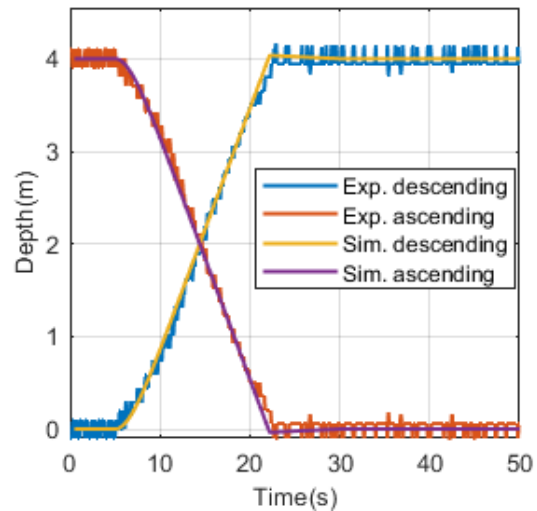
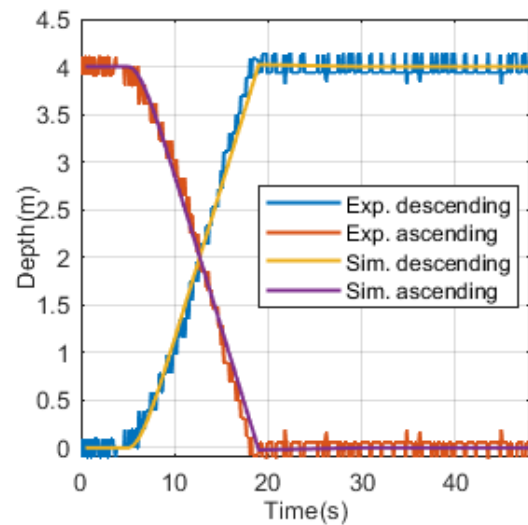


Figure 4. Experimental ascending and descending profile for  $\Delta B = 0.2$  kg, 0.4 kg and 0.6 kg for 5.0 m operating depth of the VBS in standalone mode.



(b)  $\Delta B = 0.4$  kg

Similarly, in the standalone mode, the devolved VBS ascends from 5 m depth to the surface with the same increase in buoyancy and the same time to surface. A comparative study of the simulation and experimental results for the operating depth of 4 m in ascending and descending profiles for the buoyancy change of  $\Delta B = 0.2$  kg, 0.4 kg and 0.6 kg are shown in Fig. 5. From these results of Fig. 5 (a), it can be seen that the devolved VBS rises and descends 4.0 m depth in about 24 s, i.e., at an average lifting velocity of 0.17 m/s, for a buoyancy change of  $\Delta B = 0.2$  kg (i.e., both positive and negative).



(c)  $\Delta B = 0.6$  kg

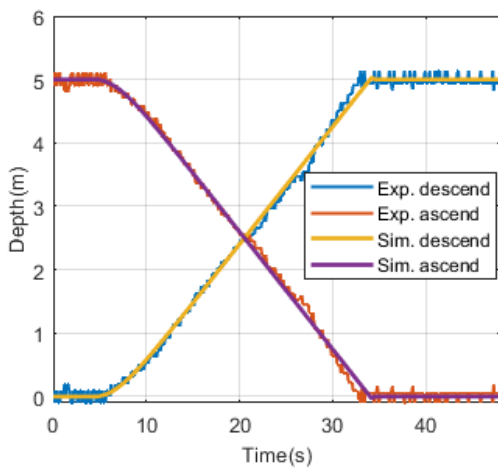
Similarly, Fig. 5 (b) and Fig. 5 (c) show the comparison of experiment and simulation for the change in buoyancy of the  $\Delta B = 0.4$  kg and 0.6 kg, respectively, for 4.0 m depth. From the simulation and experimental results in Fig. 5 (b), it can be observed that the average lifting speed for a buoyancy change of  $\Delta B = 0.4$  kg is 0.23 m/s. Both results show that the obtained performances are satisfactory.

Figure 5. Ascending and descending profile for simulation and experimental for 4 m depth at (a)  $\Delta B = 0.2$  kg and (b)  $\Delta B = 0.4$  kg and (c)  $\Delta B = 0.6$  kg change in buoyancy of the VBS in standalone mode.

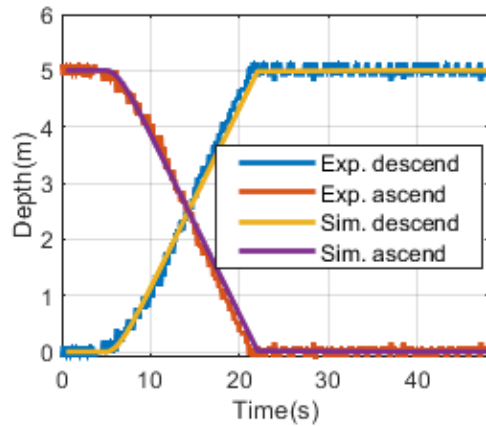
Similarly, from the results of Fig. 5 (c), it can be seen that it takes almost 13 s to rise from 4 m to the surface or to descend from the surface to a depth of 4 m (i.e., with an average heave speed of 0.3 m/s), by changing the buoyancy  $\Delta B = 0.6$  kg. Similarly, Fig. 6 shows the comparison of simulation and experimental results of the developed VBS in standalone mode for 5 m depth in ascending and descending profiles for the buoyancy changes  $\Delta B = 0.2$  kg, 0.4 kg and 0.6 kg.

From Fig. 6(a), it can be seen that for the 0.2 kg change in buoyancy (i.e., both positive and negative) of the VBS in standalone mode, the time for ascent/descent at 5 m depth is almost 30 s (i.e., at an average velocity of 0.17 m/s as before). However, since the change in buoyancy remains the same, therefore it is taking a larger time is required to reach the target depth. From Fig. 6(b), it can be seen that the ascent/descent time is 21 s to reach the surface from 5 m depth or from the surface to 5 m depth (i.e., at an average heave speed of 0.23 m/s), with the buoyancy change  $\Delta B = 0.4$  kg. Fig. 6(c) shows the ascent/descent profile of the developed VBS. From this, it can be seen that the time to reach the surface from 5 m depth or from the surface to 5 m depth is about 17 s (i.e., at an average heave speed of 0.3 m/s) due to the 0.6 kg change in buoyancy and shows the satisfactory performance compared with the simulation results.

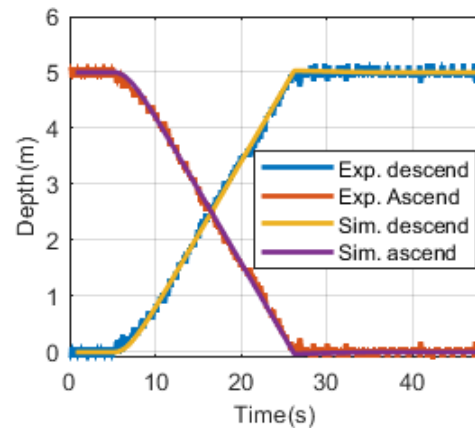
Fig. 7 (a) shows the results of the time required to descend to the different depths based on simulation and experiment for 5 trials for the  $\Delta B = 0.2$  kg change in the buoyancy of the VBS in standalone mode. Based on these results, we can observe that as the desired depth increases, the descent time also increases. This is because the system has a constant descent/ascension rate for the same change in buoyancy. Fig. 7 (b) shows the results for the buoyancy change of  $\Delta B = 0.4$  kg and the descent time for different depths by simulation and experiments for 5 series of experiments. From these results, it can be seen that all simulation results reach the desired depth with a maximum change in time of +/- 1 s.



(a)  $\Delta B = 0.2$  kg



(b)  $\Delta B = 0.4$  kg



(c)  $\Delta B = 0.6$  kg

Figure 6. Ascending and descending profile for simulation and experimental for 5 m depth at (a)  $\Delta B = 0.2$  kg and (b)  $\Delta B = 0.4$  kg and (c)  $\Delta B = 0.6$  kg change in buoyancy of the VBS in standalone mode.

The variation of depth versus time is linear, which implies that the ascending/descending average heave speed of the VBS in standalone mode is constant (i.e., 0.23 m/s) with same amount of change in buoyancy. Similarly, Fig. 7 (c) shows the change in time versus descent depth for a 0.6 kg change in buoyancy. Boxplots for experimental performance (for the 5 number of trials) for 0.6 kg change in buoyancy compared to simulation results are shown here.

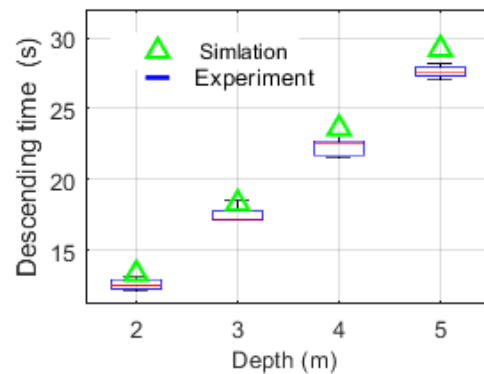


Figure 7(a): for  $\Delta B = 0.2$  kg of the VBS in standalone mode.

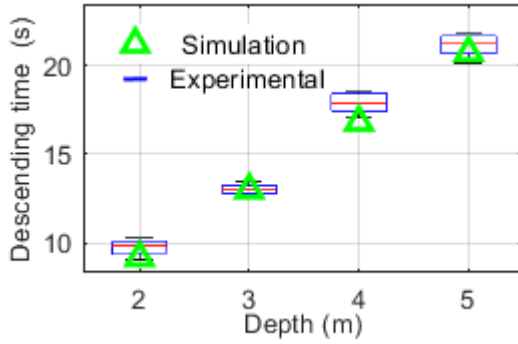


Figure 7(b): for  $\Delta B = 0.4$  kg of the VBS in standalone mode.

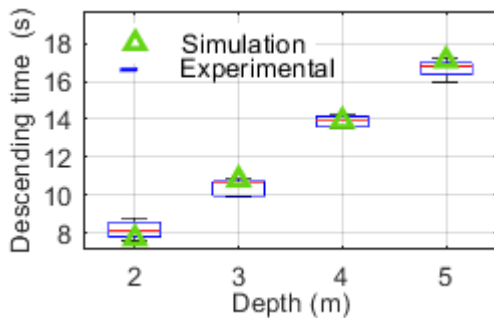


Figure 7(c): for  $\Delta B = 0.6$  kg of the VBS in standalone mode.

Figure 7. Time taken for descending to various depth with simulation and experimental (for number of trials) for change in buoyancy  $\Delta B = 0.2$  kg,  $0.4$  kg and  $0.6$  kg of the VBS in standalone mode.

Based on these results, it can be concluded that the simulation and experimental results for the number of trials show good agreement with the simulation results and the maximum time difference is 2 s to achieve the desired depth for all the number of trials.

#### 4.1 LINEAR REGRESSIONS ANALYSIS TO PREDICT THE HEAVE VELOCITY FOR SPECIFIC CHANGE IN BUOYANCY

For the experimental results of the buoyancy system and the variation of depth with time for some specific changes in buoyancy capacities, we use a machine learning algorithm (ML) for linear regression and aim to predict the optimal ascent/descent rate of the VBS using the gradient descent optimization method. Following Efron et al. (2016), for the Linear Regression (LR), a hypothesis  $h_{\theta}(\bar{x})$  is defined as follows:

$$h_{\theta}(\bar{x}) = \theta_0 + \theta_1 \bar{x} \quad (11)$$

Where  $h_{\theta}(\bar{x})$  is the hypothesis (i.e. predicted value),  $\bar{x}$  is the input features (independent variable), and  $(\theta_1, \theta_0)$  is the parameter which needs to be trained so that the error function  $(h_{\theta}(\bar{x}) - \bar{y})$  is minimized. Here,  $\bar{y}$  is the output feature (i.e. variables), and to compute the total error

we define an error function in terms of the cost function  $J(\theta_0, \theta_1)$  and that is given as follows:

$$J(\theta_0, \theta_1) = \frac{1}{2n_t} \sum_{i=1}^m (h_{\theta}(\bar{x}) - \bar{y})^2 \quad (12)$$

where  $n_t$  is the number of training data, and all the other parameters are same as defined in the previous parts. To minimize the error between the predicted value and true value of the output feature, we need to optimize the cost function  $J$  using the gradient descent algorithm by updating the parameters  $(\theta_0, \theta_1)$  which are given as follows:

$$\theta_0 = \theta_0 - \alpha \frac{\partial}{\partial \theta_0} J(\theta_0, \theta_1) = \theta_0 - \frac{\alpha}{n_t} \sum_{i=1}^m (\theta_0 + \theta_1 \bar{x}_i - \bar{y}_i) \bar{x}_i \quad (13)$$

$$\theta_1 = \theta_1 - \alpha \frac{\partial}{\partial \theta_1} J(\theta_0, \theta_1) = \theta_1 - \frac{\alpha}{n_t} \sum_{i=1}^m (\theta_0 + \theta_1 \bar{x}_i - \bar{y}_i) \bar{x}_i \quad (14)$$

where  $\alpha$  is the learning rate and all other parameters are same as defined in the previous parts. We implement the algorithm in Python to calculate the linear model for 3 different buoyancy of the developed VBS. Fig. 8 (a) shows the variation of depth versus time of the true data of the sensor and the linear regression for  $\Delta B = 0.2$  kg buoyancy change. Fig. 8 (b) shows the variation of the cost function versus number of iterations. Here, the learning rate is also referred to as the tuning parameter, because if a large value of the  $\alpha$  is chosen, the cost function may not reach its minimum value, as it first decreases for a few iterations and then increases without reaching its global minimum. Moreover, the computational cost is very high if we choose a very small value for  $\alpha$ . Therefore, we need to choose  $\alpha$  in an appropriate way to ensure that there is a good match between the accuracy and the computational cost.

Here we have chosen learning rate  $\alpha = 0.001$ , and the optimal value of the parameter obtained for the hypothesis using linear regression with the gradient descent algorithm is:  $h_{\theta}(t) = 0.18t - 0.34$ . This implies that the achieved descent rate is  $0.18$  m/s and  $0.34$  is the distorted value for the same.

Fig. 9(a) shows the variation of depth vs. time for the experimental data achieved from the sensor (i.e. true value) and the linear regression model for  $\Delta B = 0.4$  kg change in the buoyancy. Fig. 9(b) shows the cost function vs. number of iterations. In this case appropriate learning rate  $\alpha = 0.001$  and the optimum value of parameter achieved for hypothesis using the linear regression with gradient descent algorithm is:  $h_{\theta}(t) = 0.25t - 0.32$ . This implies that the descent speed achieved with linear regression model using descent gradient algorithm is  $0.25$  m/s and  $0.32$  is the biased term.

Fig. Figure 10(a) illustrates the variation of depth vs. time for the experimental data obtained from the sensor (i.e. true

value) and the linear regression model for 0.6 kg buoyancy change. Fig. 10(b) shows the cost function vs. the number of iterations for the same. Additionally, from Fig. 10(b) we can observe that as the number of iterations increases the cost function decreases and after 9 iterations it reaches the minimum. In this case, the learning rate value of 0.002 is appropriate. The optimum value of parameter achieved for hypothesis using the linear regression with gradient descent algorithm is:  $h_{\theta}(t) = 0.33t - 0.06$ . This implies that the descent speed achieved is 0.33 m/s and 0.06 is the biased term. Finally, Table 4 shows the comparison of heave speed obtained through simulation and linear regression of experimental data for various buoyancy changes. From these results we observe that the heave velocities for all the three buoyancy changes agree and match closely.

#### 4.2 EVALUATING THE PERFORMANCE OF LINEAR REGRESSION MODEL

For evaluating the performance of the linear regression model the most common method can be used is Root Mean Square Error (RMSE). RMSE can be computed by using the following formula:

$$RMSE = \sqrt{\frac{\sum_{i=1}^n (y_i - \hat{y})^2}{n}} \quad (15)$$

Where  $\hat{y}$  is predicted value of the model and  $y_i$  is actual observation values and  $n$  is the number of the observations. From Equation (15) we can note that for a better model the RMSE value will be lower and vice-versa. In this study we have computed the RMSE for three different cases of buoyancy change and for that linear regression analysis is shown in Fig. 8 to Fig. 10.

Computed RMSE values are shown in Table 4. From the Table 4 we can note that RMSE value of the regression model for 0.2 kg change in buoyancy are 0.10 and for 0.6 kg change in buoyancy are 0.16.

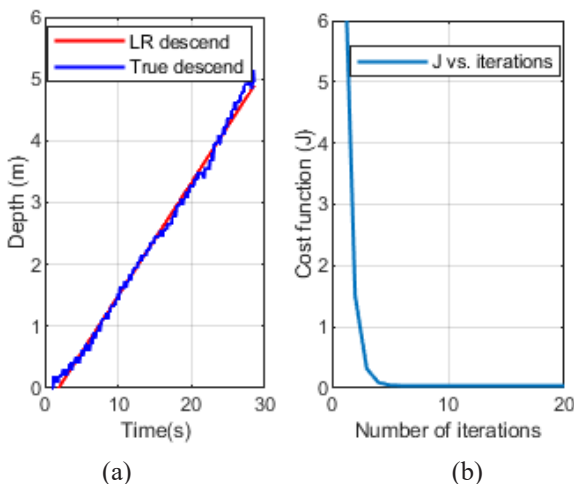


Figure 8. (a) Variation of the depth vs. time true value and using the linear regression; and (b) Cost function vs. number of iterations for  $\Delta B = 0.2$  kg change in the buoyancy.

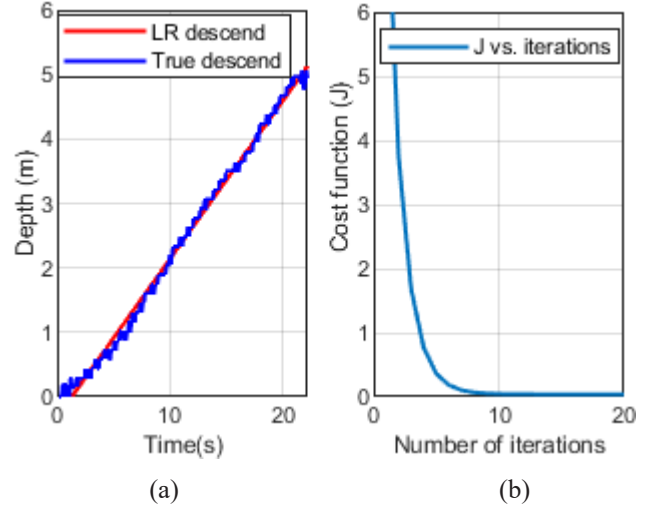


Figure 9. (a) Variation of the depth vs. time true value and using the linear regression; and (b) Cost function vs. number of iterations for  $\Delta B = 0.4$  kg change in the buoyancy.

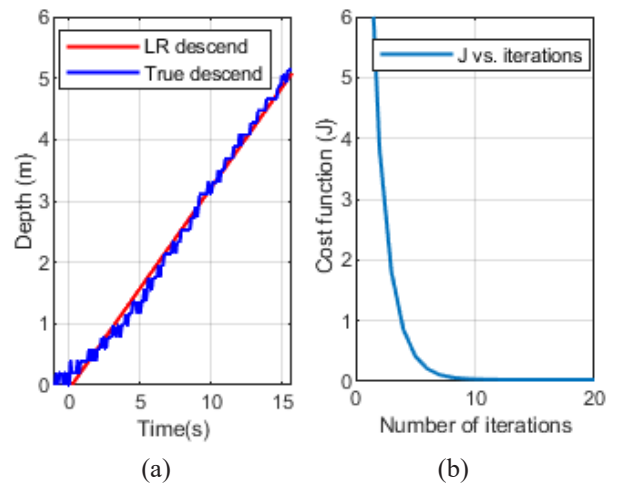


Figure 10. (a) Variation of the depth vs. time true value and using the linear regression; and (b) Cost function vs. number of iterations for  $\Delta B = 0.6$  kg change in the buoyancy.

Based upon the results we conclude that the performance of our developed VBS in standalone mode is satisfactory and it establishes the ‘Proof of Concept (PoC)’, unequivocally.

Table 4: List of the achieved heave speeds through simulation and experiments along with their linear regression analysis values and RMSE for various buoyancy changes.

$\Delta B$	Simulation heave velocity (m/s)	Linear regression of heave velocity (m/s)	RMSE
0.2 kg	0.17	0.18	0.10
0.4 kg	0.23	0.25	0.12
0.6 kg	0.30	0.33	0.16

## 5. CONCLUSIONS

In this paper, the complete design and development of the VBS in standalone mode is presented. Experiments are conducted to test the performance of the developed VBS, and the experimental results are compared with the simulation results to validate the developed VBS. In addition, the linear regression analysis is investigated and the performance of the LRM is evaluated based on the root mean square error (RMSE) of the LRM. In this study, the presented buoyancy system is tested in standalone mode and shows good performance compared with the simulation results. The performance of the developed buoyancy system is satisfactory and it is capable of operating to a depth of 60 m, but it was only tested to a depth of 5 m due to the limited test facilities available. The performance at higher depth and the UV system integrated with the developed VBS needs further investigation in the future.

## 6. ACKNOWLEDGEMENTS

This research was supported by the internal research grants of IIT madras through research scheme: OE14D212 and from Marine Systems Panel, NRB, India via a sponsored project: NRB-263/MAR/12-13

## 7. REFERENCES

1. GRIFFITHS, G. (2002) *The Technology and Applications of Autonomous Underwater Vehicles*. Taylor & Francis., London. ISBN 0-415-30154-8.
2. DESSET, S., DAMUS, R., HOVER, F., MORASH, J. and POLIDORO, V. (2005) *Closer to deep underwater science with ODYSSEY IV class Hovering Autonomous Underwater Vehicle (HAUV)*. Europe Oceans, France, pp. 758-762, doi: 10.1109/OCEANSE.2005.1513151
3. EFRON, B. and HASTIE, T. (2016) *Computer age statistical inference: algorithms, evidence, and data science*. Institute of mathematical statistics monographs, Cambridge University Press, doi:10.1017/CBO9781316576533
4. FOSSEN, T. I. (1994) *Guidance and control of ocean vehicles*. John Wiley & Sons, USA.
5. HUANG, H., ZHANG, C., DING, W., ZHU, X., SUN, G. and WANG, H. (2020) *Design of the depth controller for a floating ocean seismograph*. Journal of Marine Science and Engineering, Vol. 8(3), pp. 1-16, doi: <https://doi.org/10.3390/jmse8030166>
6. HYAKUDOME, T., AOKI, T., MURASHIMA, T., NAKAJOH, H., TSUKIOKA, S., IDA, T., MAEDA, T. and ICHIKAWA, T. (2002) *Buoyancy control for deep and long cruising range AUV*. In The Twelfth International Offshore and Polar Engineering Conference. International Society of Offshore and Polar Engineers, pp. 325-329.
7. KOBAYASHI, T., AMAIKE, K., WATANABE, K., INO, T., ASAKAWA, K., SUGA, T., KAWANO, T., HYAKUDOME, T. (2011) *Deep NINJA: A new float for deep ocean observation developed in Japan*. IEEE Symposium on Underwater Technology and Workshop on Scientific Use of Submarine Cables and Related Technologies, Tokyo, Japan, pp. 1-6, doi: 10.1109/UT.2011.5774103.
8. KOJIMA, J., KATO, Y., ASAKAWA, K., MATUMOTO, S., TAKAGI, S. and KATO, N. (1997) *Development of autonomous underwater vehicle 'AQUA EXPLORER 2' for inspection of underwater cables*. In Proceedings of MTS/IEEE Oceans, Halifax, Canada, pp. 1007-1012.
9. RANGANATHAN, T., SINGH, V., NAIR, R. and THONDIYATH, A. (2017) *Design of a controllable variable buoyancy module and its performance analysis as a cascaded system for selective underwater deployment*. Proceedings of the Institution of Mechanical Engineers, Part M: Journal of Engineering for the Maritime Environment, Vol. 231(4), pp. 888-901. doi: <https://doi.org/10.1177/1475090216688819>
10. SHIBUYA, K. and YOSHII, S. (2013) *New volume change mechanism using metal bellows for buoyancy control device of underwater robots*. International Scholarly Research Notices, pp. 1-7, doi: 10.5402/2013/541643
11. SUMANT, B., KARSITI, M.N. and AGUSTIAWAN, H. (2008) *Development of variable ballast mechanism for depth positioning of spherical URV*. International Symposium on Information Technology, Kuala Lumpur, pp.1-6, doi: 10.1109/ITSIM.2008.4631898.
12. TANGIRALA, S. and DZIELSKI, J. (2007) *A variable buoyancy control system for a large AUV*. IEEE Journal of Oceanic Engineering, Vol. 32(4), pp. 762-771. doi: 10.1109/JOE.2007.911596
13. THORLEIFSON, J. M., DAVIES, T. C., BLACK, M. R., HOPKIN, D. A., VERRALL, R. I., POPE, A., MONTEITH, I., HERTOGE, V. D. and BUTLER, B. (1997) *The Theseus autonomous underwater vehicle. A Canadian success story*. Oceans' 97. MTS/IEEE Conference Proceedings, pp. 1001-1006.
14. TIWARI, B. K. and SHARMA, R. (2020) *Design and analysis of a variable buoyancy system for efficient hovering control of underwater vehicles with state feedback controller*. Journal of Marine Science and Engineering, Vol. 8(4), pp. 1-31. doi: 10.3390/jmse8040263
15. TIWARI, B. K. and SHARMA, R. (2021) *Numerical and experimental investigation of variable buoyancy system for autonomous*

- underwater vehicle*. The Transactions of The Royal Institution of Naval Architects (Transactions RINA Part A)-International Journal Maritime Engineering, Vol. 163(A1), pp. A87-A100, doi:10.3940/ijme.2021.a1.647.
16. TIWARI, B. K. and SHARMA, R. (2021) *Study on system design and integration of variable buoyancy system for underwater operation*. Defense Science Journal, Vol. 71(1), pp. 124-133, doi: 10.14429/dsj.71.15557
  17. VBS TESTING (2021), website address: <https://www.youtube.com/watch?v=m-Yyemmet8g>
  18. WEBB, D.C., SIMONETTI, P.J. and JONES, C.P. (2001) *SLOCUM: an underwater glider propelled by environmental energy*. IEEE J. Oceanic Engineering, Vol. 26(4), pp. 447-452, doi: 10.1109/48.972077.
  19. WOODS, S. A., BAUER, R. J. and SETO, M. L. (2012) *Automated ballast tank control system for autonomous underwater vehicles*. IEEE Journal of Oceanic Engineering, Vol. 37(4), pp. 727-739, doi: 10.1109/JOE.2012.2205313.
  20. WORALL, M., JAMIESON, A. J., HOLFORD, A., NEILSON, R. D., PLAYER, M. and BAGLEY, P. M. (2007) *A variable buoyancy system for deep ocean vehicles*. OCEANS 2007 - Europe, Aberdeen, pp. 1-6, doi: 10.1109/OCEANSE.2007.4302317.
  21. ZHAO, W., XU, J. and ZHANG, M. (2010) *A variable buoyancy system for long cruising range AUV*. International Conference on Computer, Mechatronics, Control and Electronic Engineering, Changchun, pp. 585-588, doi: 10.1109/CMCE.2010.5610369.

